Applied Surface Science 257 (2011) 4321–4324

Contents lists available at ScienceDirect

Applied Surface Science

journal homepage: www.elsevier.com/locate/apsusc

Abrupt transition from wavelength structure to subwavelength structure in a single-crystal superalloy induced by femtosecond laser

Wei Zhang[a,b], Guanghua Cheng[b], Qiang Feng[a,c,*], Lamei Cao[d], Fengping Wang[e], Rongqing Hui[f]

[a] State Key Laboratory for Advanced Metals and Materials, University of Science and Technology Beijing, Beijing 100083, China
[b] State Key Laboratory of Transient Optics and Photonics, Xi'an Institute of Optics and Precision Mechanics of Chinese Academy of Sciences, Xi'an Shaanxi 710119, China
[c] National Center for Materials Service Safety, University of Science and Technology Beijing, Beijing 100083, China
[d] National Key Laboratory of Science and Technology on Advanced High Temperature Structural Materials, Beijing Institute of Aeronautical Materials, Beijing 100095, China
[e] Applied Science School, University of Science and Technology Beijing, Beijing 100083, China
[f] Department of Electrical Engineering and Computer Science, University of Kansas, Lawrence, KS 66044, USA

ARTICLE INFO

Article history:
Received 24 November 2010
Accepted 8 December 2010
Available online 17 December 2010

Keywords:
Femtosecond laser
Microstructure
Abrupt transition
Second harmonic generation

ABSTRACT

The abrupt transition from low-spatial-frequency laser-induced periodic surface structure (LSFL) to high-spatial-frequency laser-induced periodic surface structure (HSFL) in single-crystal superalloy CMSX-4 during femtosecond laser irradiation has been reported. Microstructural investigations indicate that the transition was initiated by the generation of new grooves on the main ridges of LSFL ripples. This transition resulted in the period of HSFL nearly equal to half of LSFL period. Furthermore, the relationship between both LSFL and HSFL and their parametric dependence was established. The microstructural observation of the abrupt transition provides a morphological evidence of second harmonic generation being responsible for the formation of HSFL.

1. Introduction

Most laser-induced periodic surface structures (LIPSS) are the wavelength-scale ripple structure, usually referred to low-spatial-frequency LIPSS (LSFL), and they have been observed on most materials. It is generally accepted that this type of wavelength-scale LSFL arises from effects of optical interference due to coherent interaction between the incident radiation and surface scattered electromagnetic wave [1,2]. However, recent studies suggest that another type of LIPSS with the spatial period much less than the incident laser wavelength (λ) was produced by femtosecond laser irradiation on various solids, and it is referred to high-spatial-frequency LIPSS (HSFL) [3–8]. There are two main mechanisms proposed for the formation of the HSFL. One is involved in the interaction of incident laser pulses with laser-produced surface plasma, in which the period (Λ) of LIPSS was dependent on the laser fluence [3,8]. For instance, the ripple period was found to decrease with the laser fluence on the surface of copper [3]. Another mechanism is associated with the combination of interference effects and second harmonic generation (SHG) [4–7]. According to this model, the HSFL period was given by $\Lambda = \lambda/2$ for strongly absorbing materials such as metals and $\Lambda = \lambda/2n$ (n is the refractive index of materials) for transparent materials under normal incident irradiation. To date, the process for the formation of the HSFL is still not well understood, and further experimental and theoretical studies are required.

In the current study, the LIPSS on the surface of a single-crystal superalloy after irradiation by a femtosecond laser with various levels of laser fluence and nominal pulse number was investigated. The characteristics of both LSFL and HSFL and the direct correlation between them have been identified by microstructural investigation. These results provide a morphological evidence of SHG being responsible for the formation of the HSFL.

2. Experimental

A chirped pulse amplification-based Ti:sapphire regenerative amplifier laser system (Spitfire, Spectra Physics) was used to generate linearly polarized laser pulses at a center wavelength of $\lambda = 800$ nm with pulse duration of $\tau = 120$ fs and a maximum repetition rate of 1 kHz. The laser beam was perpendicular to the sample surface and focused using a 5× microscope objective lens with 0.14NA (Mitutoyo). The energy of the laser incident radiation was varied using a polarizer combined with a half wave plate. The sample was mounted on a computer-controlled *xyz* translation stage with a spatial resolution of 125 nm, and the experiments were carried out by translating the sample relatively to the stationary laser

* Corresponding author at: State Key Laboratory for Advanced Metals and Materials, University of Science and Technology Beijing, 30 Xueyuan Road, Beijing 100083, Haidian District, China. Tel.: +86 10 62333584; fax: +86 10 62329915.
E-mail address: qfeng@skl.ustb.edu.cn (Q. Feng).

0169-4332/$ – see front matter © 2010 Elsevier B.V. All rights reserved.
doi:10.1016/j.apsusc.2010.12.050

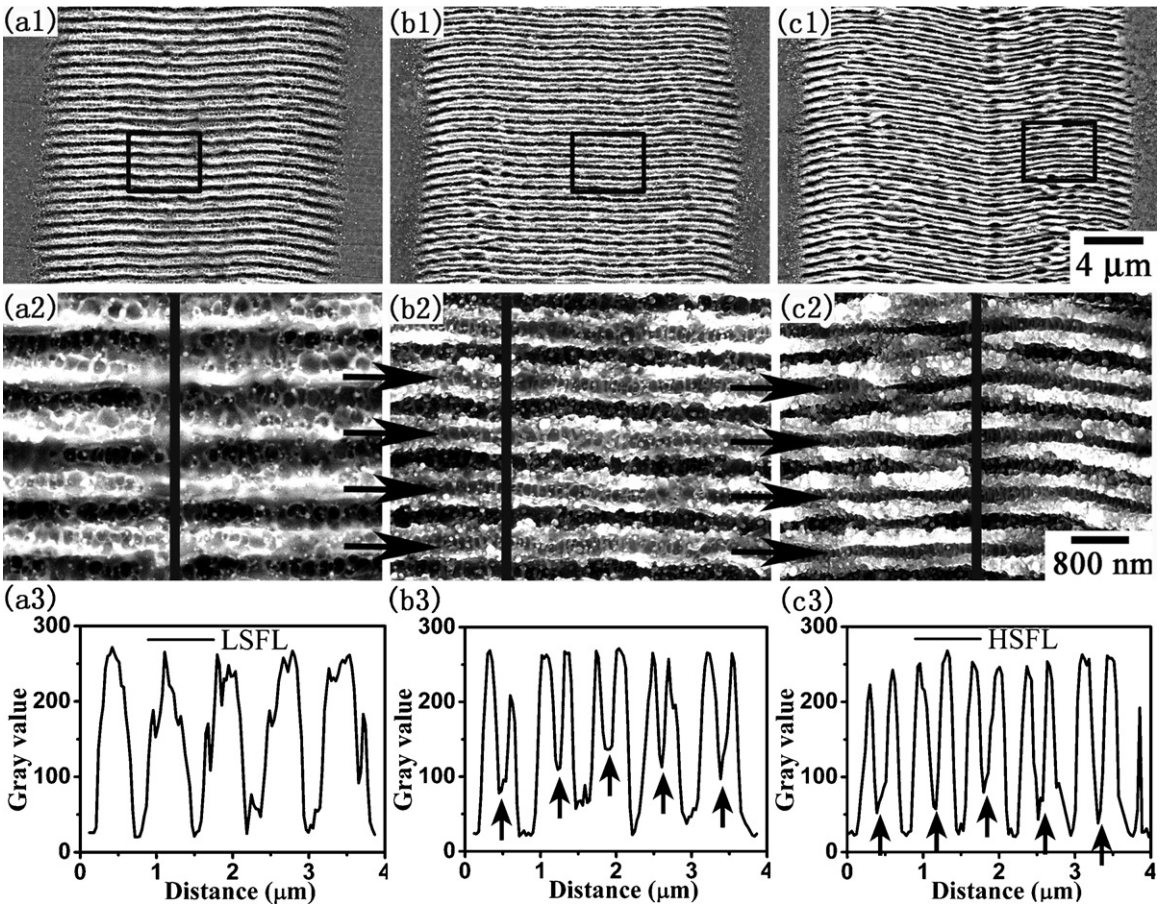

Fig. 1. Typical microstructures of LIPSS on the surface of single-crystal superalloy CMSX-4 after femtosecond laser irradiation with three feedrates at the constant laser fluence $\Phi = 0.82\,J/cm^2$. (a) Feedrate $\nu = 3.75$ mm/s ($N \sim 9$), (b) $\nu = 1.25$ mm/s ($N \sim 26$), (c) $\nu = 0.625$ mm/s ($N \sim 52$); (a2), (b2) and (c2) show higher magnification images of the framed area in (a1), (b1) and (c1), respectively; (a3), (b3) and (c3) show gray value profiles along the trace path in (a2), (b2) and (c2), respectively.

beam with the feedrates (ν) varying between 0.125 and 16 mm/s in the direction perpendicular to the incident laser beam. The corresponding nominal pulse number (N) was calculated based on the feedrate and the focused beam diameter (~32 μm). All experiments were carried out in ambient air.

The sample used in the experiment was a second-generation single-crystal superalloy, CMSX-4. The surface of the selected sample was polished by conventional metallographic procedures with a final polish of 0.05 μm suspended alumina powder. Before and after laser processing, the sample was subjected to ultrasonic cleaning in ethanol for 5–10 min. The morphology of the laser-induced periodic microstructure was examined by a ZEISS SUPRA 55 field-emission scanning electron microscope (FE-SEM) operated in secondary electron (SE) imaging mode. Some critical LIPSS were investigated using an Agilent Technologies 5500 atomic force microscope (AFM) in order to determine the amplitude of the ripples. The LIPSS period was measured with the help of ImageJ program, which was created at the National Institutes of Health, USA [9].

3. Results

Fig. 1(a–c) shows the typical microstructures of LIPSS on the surface of the single-crystal superalloy CMSX-4 after femtosecond laser irradiation with three feedrates at the constant laser fluence $\Phi = 0.82\,J/cm^2$. This fluence level was approximately 2.5 times higher than the ablation threshold for single-crystal superalloy MK-4, which has similar composition to CMSX-4 [10]. In all cases, femtosecond-LIPSS have been observed and the orientation of the ripples was perpendicular to the polarization of the 800 nm laser radiation. Fig. 1(a2–c2) shows higher magnification images of the framed area in Fig. 1(a1–c1), respectively and Fig. 1(a3–c3) shows the gray value profiles along the trace path in Fig. 1(a2–c2), respectively. The microstructures clearly demonstrate the morphological evolution of LIPSS. After irradiation with $\nu = 3.75$ mm/s ($N \sim 9$), periodic ripples of classical LSFL were observed with the period of ~760 nm approximately equal to the wavelength of the incident laser (Fig. 1(a2–a3)). With decreasing levels of the feedrate, new grooves marked by arrows appeared on the main ridges of the ripples as shown in Fig. 1(b2–b3). When the feedrate was decreased to 0.625 mm/s ($N \sim 52$), these new grooves became more distinctive and the dominant feature of the HSFL demonstrated with a shorter period of ~360 nm (Fig. 1(c2–c3)), which was nearly half of the LSFL period.

In order to better understand the process of transforming from the LSFL into the HSFL, the intermediate structure produced with $\nu = 1.25$ mm/s ($N \sim 26$) as shown in Fig. 1(b1–b3) was further investigated using AFM. Fig. 2(a) is a typical AFM 3-D profile image of this intermediate structure, while Fig. 2(b) shows the higher magnification image of the framed area in Fig. 2(a). Mixed characteristics of both LSFL and HSFL were observed in this intermediate structure. It is clearly demonstrated that each main ridge along the LSFL ripples with a space of 760 nm (Fig. 2(a)) started to split into two ridges with a new groove in some ripple area (Fig. 2(b)). The cross-section profiles along the upper path and the lower path were shown in Fig. 2(c). Compared with the LSFL ridges along the upper path, new grooves masked by arrows in Fig. 2(c) were generated on the ripple

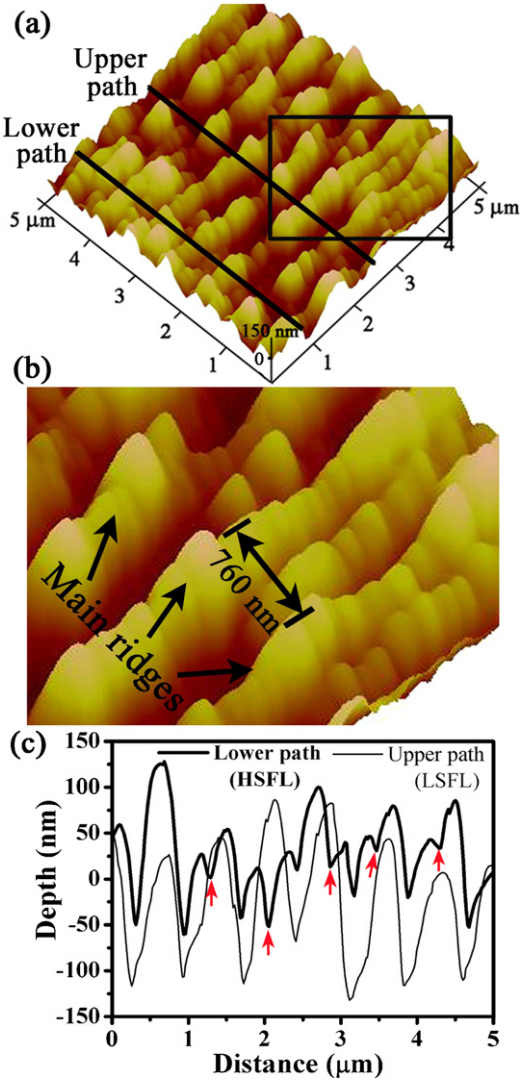

Fig. 2. AFM analyses of the surface for single-crystal superalloy CMSX-4 after femtosecond laser irradiation with feedrate $v = 1.25$ mm/s ($N \sim 26$) at the laser fluence $\Phi = 0.82$ J/cm^2. (a) AFM 3-D profile image; (b) higher magnification image of the framed area in (a); (c) cross-section profile for lower (HFSL) and upper (LFSL) path in (a).

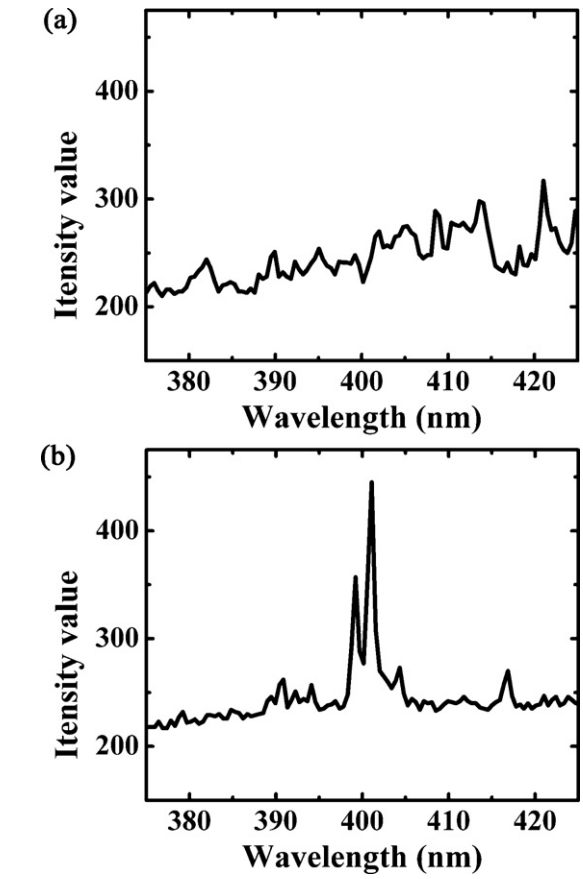

Fig. 3. Wavelength distribution scattered from the irradiated surface of single-crystal superalloy CMSX-4 at the constant laser fluence $\Phi = 0.82$ J/cm^2 with (a) $v = 3.75$ mm/s ($N \sim 9$); (b) $v = 0.625$ mm/s ($N \sim 52$). The chosen experimental conditions are the same as Fig. 1(a) and (c), respectively.

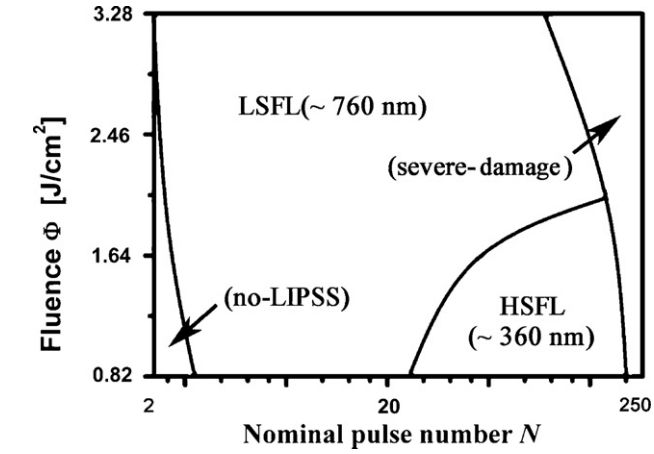

Fig. 4. Occurrence of LIPSS on the surface of single-crystal superalloy CMSX-4 after femtosecond laser irradiation with respect to nominal pulse number and laser fluence.

ridges along the lower path where most of the HSFL were located, leading to $\Lambda_{HSFL} \sim \Lambda_{LSFL}/2$.

Fig. 3(a) and (b) shows the optical spectra of the scattered light from the irradiation area on the sample surface under two experimental conditions, which are the same as those to produce typical LSFL and HSFL, respectively, as shown in Fig. 1(a) and (c). It is demonstrated that the discrete wavelength component at 400 nm was only observed in the experimental condition where the HSFL was predominantly visible as shown in Fig. 1(c1–c3). In the current stage, the observed wavelength component of 400 nm is expected to produce due to SHG.

Furthermore, the LIPSS on the surface of the single-crystal superalloy CMSX-4 after femtosecond laser irradiation have also been investigated with various levels of laser fluence and nominal pulse number. Fig. 4 is a map of the relationship among LIPSS, laser fluence and nominal pulse number. The intermediate structure is regarded as the HSFL in this map since it is very difficult to distinguish the boundary between the intermediate structure and the HSFL. The following characteristics have been identified in this map: (1) it has been divided into four-zones, consisting of no-LIPSS, LSFL, HSFL and severe-damage zone; (2) no direct transition occurred from no-LIPSS to the HSFL; (3) the formation of the HSFL is restricted to a relatively small operation region; (4) in the severe-damage zone, the surface started to be severely ablated due to large pulse number and high laser fluence, as a result, the LSFL and HSFL finally disappeared. It is worthy of noting that the transition boundary from the LSFL to the HSFL depended on the number of laser pulses and the laser fluence. For higher laser fluence ($\Phi > 2.05$ J/cm^2), the transition has not been observed at any number of laser pulses.

4. Discussion

Recently, a number of different research groups have investigated the HSFL on various solid surfaces and two main mechanisms mentioned at the exordium have been proposed for the formation of the HSFL. In the present study, there was no ripple period other than 360 nm and 760 nm in the laser fluence range between 0.82 J/cm^2 and 3.28 J/cm^2. The insensitivity of the laser fluence on the period for both LSFL and HSFL is clearly different from the previous report of continuous transitions of the ripple period with the change of the laser fluence [3]. This result effectively excludes the interaction of laser pulses and laser-produced surface plasma as a possible explanation.

In order to verify the role of the SHG in the physical origin of the HSFL, the possible relationship between the HSFL and the wavelength of an incident laser after femtosecond laser irradiation under different irradiation conditions became one of the fundamental issues [4–7]. Borowiec and Haugen reported that the period of the HSFL in III–V semiconductors (InP, GaP, GaAs) was 4.2–5.1 times less than the wavelength of the incident laser [5]. They speculated that SHG at the surface might play a key role in the formation of the HSFL. Jia et al. found the HSFL with $\Lambda \approx \lambda/2n$ on the entire ablation area of ZnSe crystal, and they attributed the formation of the HSFL to the interference between the surface scattered wave of the incident laser (800 nm) and its second harmonics at 400 nm [7]. Bonse et al. observed the period of the HSFL ($\Lambda \sim \lambda/2$) was half of that of the LSFL ($\Lambda \sim \lambda$) in single-crystalline indium phosphide (c-InP), and the observations suggested that SHG was responsible for the HSFL formation [4]. In the current study, both spatial LSFL ($\Lambda \sim 760$ nm) and HSFL ($\Lambda \sim 360$ nm) after femtosecond laser irradiation in the single-crystal superalloy were also observed. Furthermore, microstructural investigation indicate that the formation of the HSFL was initiated by the generation of the new grooves on the main ridges of the LSFL ripples, i.e., the involvement of abrupt transition from the LSFL to the HSFL, leading to $\Lambda_{HSFL} \sim \Lambda_{LSFL}/2$. And the spectroscopic results suggest that SHG was only associated with the formation of the HSFL regime. As a result, the process for HSFL generation is explained as follows: (1) second harmonic can be efficiently generated on a significant rough surface structured by the LSFL; (2) a new type of periodic modulated intensity field is formed due to the interference effect between the second harmonic and its scattered surface wave; (3) for the subsequent pulses, a positive feedback effect of this new field is created by succedent SHG, and becomes significant enough to promote the transition from the LSFL to the HSFL.

5. Conclusions

In summary, the formation of both wavelength-scale LSFL ($\Lambda_{LSFL} \sim 760$ nm) and subwavelength-scale HSFL ($\Lambda_{HSFL} \sim 360$ nm) has been observed in a single-crystal superalloy CMSX-4 after femtosecond laser irradiation with various levels of laser fluence and nominal pulse number. Microstructural investigations indicate that the transition from the LSFL to the HSFL was initiated by the generation of the new grooves on the main ridges of the LSFL ripples, leading to $\Lambda_{HSFL} \sim \Lambda_{LSFL}/2$. The map of the occurrence for both ripple types and their parametric dependence was established, and the formation of the HSFL only occurred in a limited range of nominal pulse number and laser fluence. The periods of both the LSFL and the HSFL are almost constant and insensitive to the laser fluence and nominal pulse number. The current results present morphological evidences to support that the HSFL were generated under the help of the nonlinear response of the LSFL, and it was due to the involvement of SHG.

Acknowledgements

The authors are very grateful to T.M. Pollock for providing materials. The financial support provided by High Technology Research and Development Program of China (No. 2007AA03A225), New Century Excellent Talents in University, Chinese Ministry of Education (Grant No.: NCET-06-0079), and the CAS/SAFEA International Partnership Program for Creative Research Teams is gratefully acknowledged.

References

[1] D.C. Emmony, R.P. Howson, L.J. Willis, Laser mirror damage in germanium at 10.6 μm, Appl. Phys. Lett. 23 (1973) 598–600.
[2] J.E. Sipe, J.F. Young, J.S. Preston, H.M. van Driel, Laser-induced periodic surface structure. I. Theory, Phys. Rev. B 27 (1983) 1141–1153.
[3] S. Sakabe, M. Hashida, S. Tokita, S. Namba, K. Okamuro, Mechanism for self-formation of periodic grating structures on a metal surface by a femtosecond laser pulse, Phys. Rev. B 79 (2009) 033404–033409.
[4] J. Bonse, M. Munz, H. Sturm, Structure formation on the surface of indium phosphide irradiated by femtosecond laser pulses, J. Appl. Phys. 97 (2005) 013538–013539.
[5] A. Borowiec, H.K. Haugen, Subwavelength ripple formation on the surfaces of compound semiconductors irradiated with femtosecond laser pulses, Appl. Phys. Lett. 82 (2003) 4462–4464.
[6] D. Dufft, A. Rosenfeld, S.K. Das, R. Grunwald, J. Bonse, Femtosecond laser-induced periodic surface structures revisited: a comparative study on ZnO, J. Appl. Phys. 105 (2009) 034908–034909.
[7] T.Q. Jia, H.X. Chen, M. Huang, F.L. Zhao, J.R. Qiu, R.X. Li, Z.Z. Xu, X.K. He, J. Zhang, H. Kuroda, Formation of nanogratings on the surface of a ZnSe crystal irradiated by femtosecond laser pulses, Phys. Rev. B 72 (2005) 125429.
[8] G. Miyaji, K. Miyazaki, Origin of periodicity in nanostructuring on thin film surfaces ablated with femtosecond laser pulses, Opt. Express 16 (2008) 16265–16271.
[9] M.D. Abramoff, P.J. Magelhaes, S.J. Ram, Image processing with ImageJ, Biophotonics Int. 11 (2004) 36–42.
[10] Q. Feng, Y.N. Picard, H. Liu, S.M. Yalisove, G. Mourou, T.M. Pollock, Femtosecond laser micromachining of a single-crystal superalloy, Scripta Mater. 53 (2005) 511–516.